

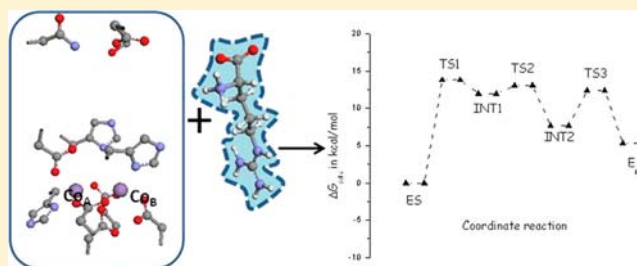
What Occurs by Replacing Mn^{2+} with Co^{2+} in Human Arginase I: First-Principles Computational Analysis

Tiziana Marino,* Nino Russo, and Marirosa Toscano

Dipartimento di Chimica and Centro di Calcolo ad Alte Prestazioni per Elaborazioni Parallele e Distribuite-Centro d'Eccellenza MURST, Università della Calabria, I-87030 Arcavacata di Rende (CS), Italy

Supporting Information

ABSTRACT: The reaction mechanism of the dinuclear cobalt enzyme arginase is investigated using density functional theory. As an arginase-containing binuclear Mn_2^{2+} cluster, it catalyzes the hydrolysis of L-arginine in L-ornithine and urea. The bridging hydroxide is capable of performing nucleophilic attack on the iminium carbon ion from its bridging position, resulting in the formation of a tetrahedral intermediate, as was already obtained in a previous theoretical study on the manganese enzyme. Our theoretical investigation allows us to obtain an accurate potential energy profile and confirms that the coordination mode of the substrate to the dimetallic center is quite similar to that present in the manganese enzyme. In agreement with the experimental observations, our results show that both Mn- and Co-containing enzymes catalyze the same reaction with quite comparable energy barriers.



INTRODUCTION

Arginases are typical metalloenzymes that require the metal ions to maintain their stable native state. These enzymes catalyze the hydrolysis of L-arginine (L-Arg) to give the nonprotein amino acid L-ornithine (L-Orn) and urea. Ornithine is a biosynthetic precursor of proline and the polyamines. Besides being in the liver, the enzyme has been discovered in different nonhepatic tissues; this fact suggested that this enzyme can be involved in functions other than those in nitrogen metabolism. The discovery of the enzyme nitric oxide synthase (NOS), which catalyzes the oxidation of arginine to NO and citrulline, roused interest in the mutual interaction between the NOS and arginase reaction paths.^{1–3}

Although the binuclear Mn^{2+} cluster in the human arginase I (hArgI) represents the physiological activator,⁴ other metal ions (Co^{2+} , Ni^{2+} , Fe^{2+} , and Cd^{2+}) have been found to satisfy the requirements for some other arginases.^{5–10} Most recently, by substitution of the Mn_2^{2+} cluster with Co_2^{2+} , an enzyme with greater activity has been obtained ($k_{\text{cat}}/K_{\text{M}}$) at the serum pH (7.4)¹¹ because of a lowered value of K_{M} for the L-Arg substrate reaction. This observation allowed us to consider Co^{2+} -arginase as a more effective agent for L-Arg depletion therapy.¹¹ In this work, Stone et al. propose a different catalytic mechanism for Co^{2+} -arginase compared with the parental enzyme in an attempt to rationalize the lower K_{M} value of L-Arg and the lower K_{i} value of L-Orn. In fact, on the basis of their findings, the authors recommended that the hydroxide ion coordinated to an unspecified Co^{2+} ion performs the nucleophilic attack to the guanidinium group bound to the other Co^{2+} ion. In this way, the stability of the tetrahedral intermediate formed is ensured by coordination of the N_{ϵ} and O_{H} atoms to the Co^{2+}

ions.¹¹ Lately an X-ray diffractometric study¹² appeared that changed radically the conclusions drawn by the previous work.¹¹ In particular, D'Antonio and Christianson¹² found that the unliganded Co^{2+} -arginase determined at both 2.10 Å (pH = 7.0) and 1.97 Å (pH = 8.5) resolution is essentially the same as the corresponding structures of Mn^{2+} -arginase. The same observations have been made on the enzyme structures bounded with the reactive substrate analogue 2(S)-amino-6-borono-hexanoic acid (ABH) and with the catalytic product L-Orn.¹¹ Because no significant structural differences are responsible for the better catalytic activity of Co^{2+} -arginase with respect to Mn^{2+} -arginase, we have hypothesized that metal substitution can affect some steps of the reaction mechanism. For this purpose, we have undertaken a quantum-chemical study of the catalytic cycle of Co^{2+} -arginase at the density functional theory (DFT) level by using the same computational protocol previously employed for elucidation of the Mn^{2+} -arginase reaction mechanism.¹³

COMPUTATIONAL DETAILS

The Becke–Lee–Yang–Parr (B3LYP) hybrid functional method,^{14–16} as implemented in the Gaussian03 program package,¹⁷ was used for optimization of all of the species along the considered reaction path. For Co atoms, the relativistic compact Stuttgart/Dresden effective core potential coupled with its split-valence basis set was used.¹⁸ The 6-31+G* basis set has been employed for the rest of the atoms. The nature of the stationary points (minimum or saddle point) has been verified by vibrational analysis performed at the same level of theory.

Received: August 2, 2012

Published: December 28, 2012

Furthermore, the intrinsic reaction coordinate procedure has been used in order to verify whether the transition states are connected to the given minima. More accurate energy values were obtained with single-point calculations on the previously optimized geometries, increasing the basis set size [6-311+G(d,p)] and including the solvent effects throughout the self-consistent-reaction-field polarizable continuum model.^{19,20} The dielectric constant was chosen as equal to 4, as is commonly used for proteins.^{13,21–31}

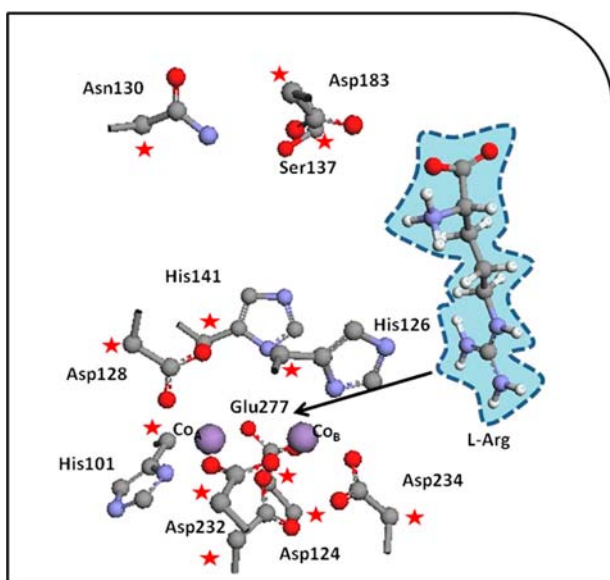
All relative energies (in kcal/mol) reported on the energetic path are Gibbs free energies in solution calculated at $T = 298.15$ K.

Analysis of the natural bonding orbitals (NBOs)³² has been performed in order to estimate the net charges within all stationary points on the potential energy surface (PES).

The quantum cluster model approach has been chosen to obtain the enzyme–substrate model, as previously made and extensively described in the case of Mn^{2+} -arginase.¹³ It consists of keeping fixed during the geometry optimizations a number of atoms with the aim of preventing unrealistic movements of the various groups in the model. This technique implicates a few small imaginary frequencies, in this case all below $60i$ cm^{-1} , that are irrelevant to the zero-point energy (ZPE) and can be ignored.^{33,34}

The X-ray structure (PDB code 1D3 V)³⁵ of rat arginase I bounded with boronic acid, a substrate analogue inhibitor, used in our previous investigation¹³ has been chosen to build the cluster employed in the present investigation. The Mn atoms were substituted by the Co ones because the structures previously deposited in the protein data bank showed that Co^{2+} substitution does not generate any important structural changes in the active site of human arginase.¹² The resulting cluster shown in Scheme 1 contains 115 atoms and has a total charge

Scheme 1. Active-Site Model of Co^{2+} -Arginase and Its Substrate (L-Arg)^a



^aStars indicate the atoms that during the optimization procedure are fixed to their X-ray positions.

of 2–. It satisfies the crucial requirements for the catalytic activity: the substrate's orientation into the active site, the protonation state, and the coordination binding mode to the dimetallic center, as attested also by the most recent work.¹²

RESULTS AND DISCUSSION

Following the previous theoretical work on Mn-containing arginase¹³ and the most recent experimental study on cobalt-reconstituted human arginase I,¹² we have considered the reaction mechanism depicted in Scheme 2.

Preliminary calculations were carried out on the ES complex with the aim of establishing the most stable spin multiplicity of the system. For this purpose, different values of spin multiplicity ($2S + 1 = 3, 5, 7,$ and 9) were taken into account. The lowest energy was obtained with a value equal to 7 because the next one ($2S + 1 = 5$) lies about 20 kcal/mol above. Furthermore, for the quintet and septet electronic spin states, we have also performed computations for the TS1 and E_p complexes. Also, for these stationary points, the lowest energy profile corresponds to the septet electronic state. For these reasons, all of the other species along the reaction path have been determined considering the septet as the electronic spin multiplicity. On the other hand, a recent study³⁶ on the $\text{Co}(\text{acac})_2$ complex, performed at DFT and CASPT2 levels of theory, clearly shows that in a tetracoordinated geometry the ground state of this system is the high spin ($2S + 1 = 4$), and for its dimer, the lowest energy corresponds to the septet.

The B3LYP potential energy profile (ΔG_{soln}) computed in the protein environment is shown in Figure 1.

The reaction starts with the formation of the ES complex between the bridging $-\text{OH}$ species in the active site of Co^{2+} -arginase with the L-Arg substrate (see Figure 2). A comparison between this structure and the ES complex in Mn-containing arginase reveals that L-Arg by its N_η^2 atom is located closer to Co^{2+}_A (2.441 Å) than to Mn^{2+}_A (2.562 Å). This means that the $-\text{OH}$ group is at a better distance with the substrate C atom (2.750 vs 2.831 Å in Mn^{2+} -arginase) and nucleophilic attack should be facilitated. A previous experimental investigation hypothesized that, because the geometrical features of the ES complexes in the two cases are similar, a way to explain the different kinetic behaviors should be derived by different electrostatic distributions in the active site.¹²

From our NBO charge analysis, no significant differences have been found. In fact, the net charges on the metal centers ($\text{Co}_A = 1.186$ |e|, $\text{Co}_B = 1.188$ |e|; $\text{Mn}_A = 1.299$ |e|, $\text{Mn}_B = 1.280$ |e|) as well as that of the O atom of the hydroxyl group (-1.114 |e| in Co^{2+} -arginase vs -1.171 |e| in Mn^{2+} -arginase) and of the carbonyl C atom of the substrate (0.730 |e| in Co^{2+} -arginase vs 0.731 |e| in Mn^{2+} -arginase) are almost the same.

Another possible explanation must consider the strength of the ES complexes. It is known that the K_M value includes the affinity of the substrate for the enzyme, and when the rate at which the substrate bound to the enzyme is converted to product (k_2) is much smaller than k_{-1} , K_M will be equal to the binding affinity. The experimentally observed K_M value of Co^{2+} -arginase is lower than that of Mn^{2+} -arginase,¹¹ meaning a higher affinity for the substrate of the Co-containing enzyme. Our computations for the enzyme–substrate affinity in the Co- and Mn-containing enzymes (167.7 and 164.8 kcal/mol, respectively) agree with the experimental evidence.¹¹

After formation of the ES complex, the reaction proceeds throughout the transition state species, TS1 (see Figure 3), with an energy demand of 15.7 kcal/mol. It describes the nucleophilic addition by the bridging $-\text{OH}$ to the iminium C ion, as confirmed by the imaginary frequency of $258.6i$ cm^{-1} associated with the O_H-C stretching mode. The O_H-C distance (1.804 Å) underlines that this bond is already formed. NBO analysis shows the σ nature of the $\text{O}-\text{C}$ bond that contains p character of 83.4% and 87.9% for O and C atoms, respectively. Also the charge values change with respect to that present on the ES complex. In fact, now the net charges on Co_A (1.153 |e|) and Co_B (1.202 |e|) appear to be differentiated and that on the O atom of the $\text{OH}-$ nucleophile species is -0.965 |e|.

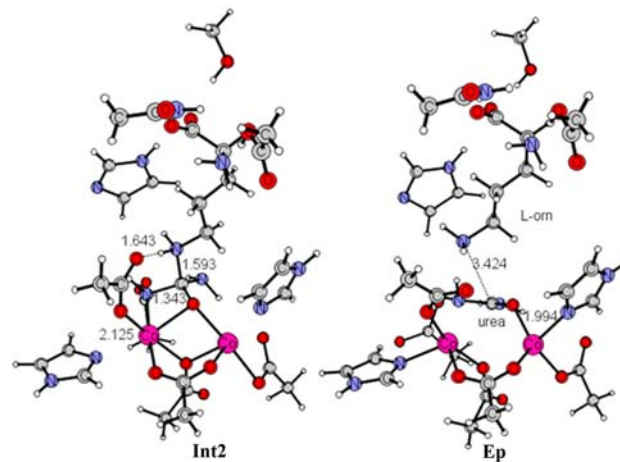
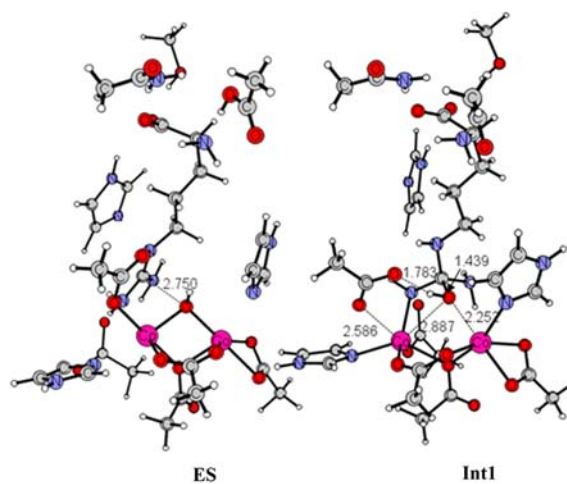
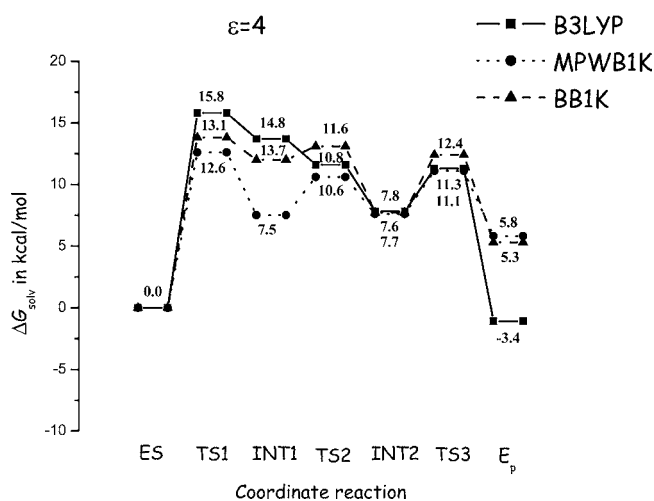
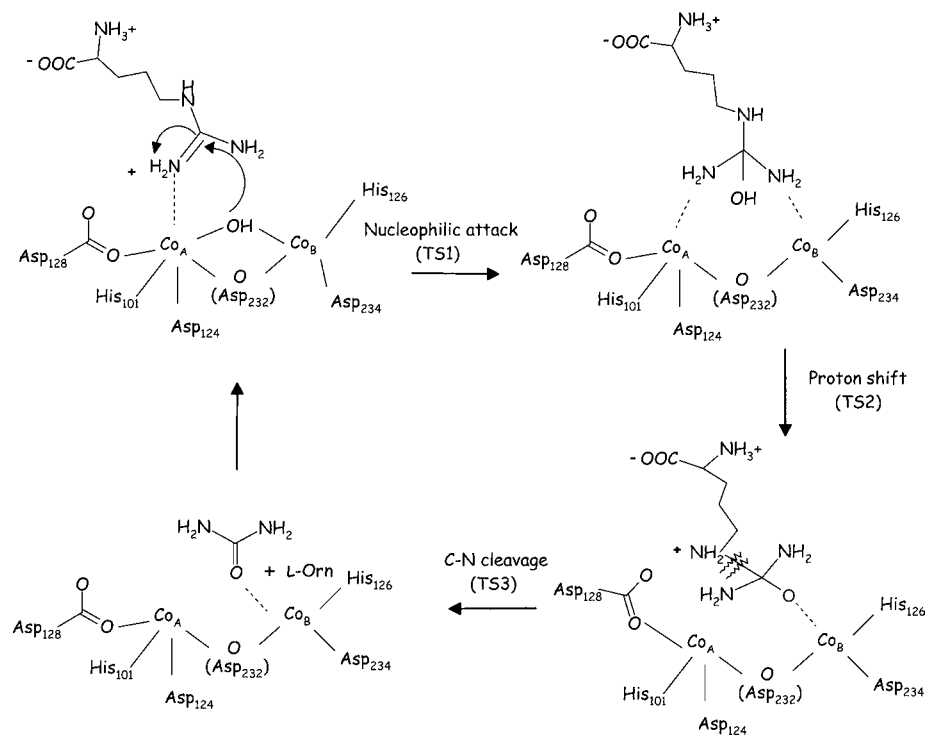
Scheme 2. Catalytic Mechanism Proposed for Co^{2+} -arginase

Figure 1. Energetic profiles of the hydrolysis mechanism of Co^{2+} -arginase.

el. Furthermore, we find a net charge of 0.779 lel on the iminium C ion and a negative charge distribution on the N_{η^1} (-0.898 lel) and N_{η^2} (-0.828 lel) atoms. Analogous information arises from NBO analysis of TS1 in Mn^{2+} -arginase as far as the orbital composition and the charge values on the active center atoms are concerned ($\text{Mn}_A = 1.281$ lel, $\text{Mn}_B = 1.308$ lel and the OH^- nucleophile = -0.977 lel), but some differences occur on the substrate atoms: $\text{N}_{\eta^1} = -0.909$ lel, $\text{N}_{\eta^2} = -0.844$ lel, and iminium C ion = 0.781 lel. These differences along with the ionic radii are also reflected in the distances $\text{Mn}_A - \text{N}_{\eta^1}$ (2.327 Å) and $\text{Co}_A - \text{N}_{\eta^1}$ (2.196 Å), which confirm that the substrate is better anchored in the enzyme containing the Co^{2+} cluster.

A comparison with the Mn-containing enzyme reveals that the substitution of Co with Mn does not affect significantly the

Figure 2. Optimized geometries of the minima along the reaction pathway. Distances are in angstroms.

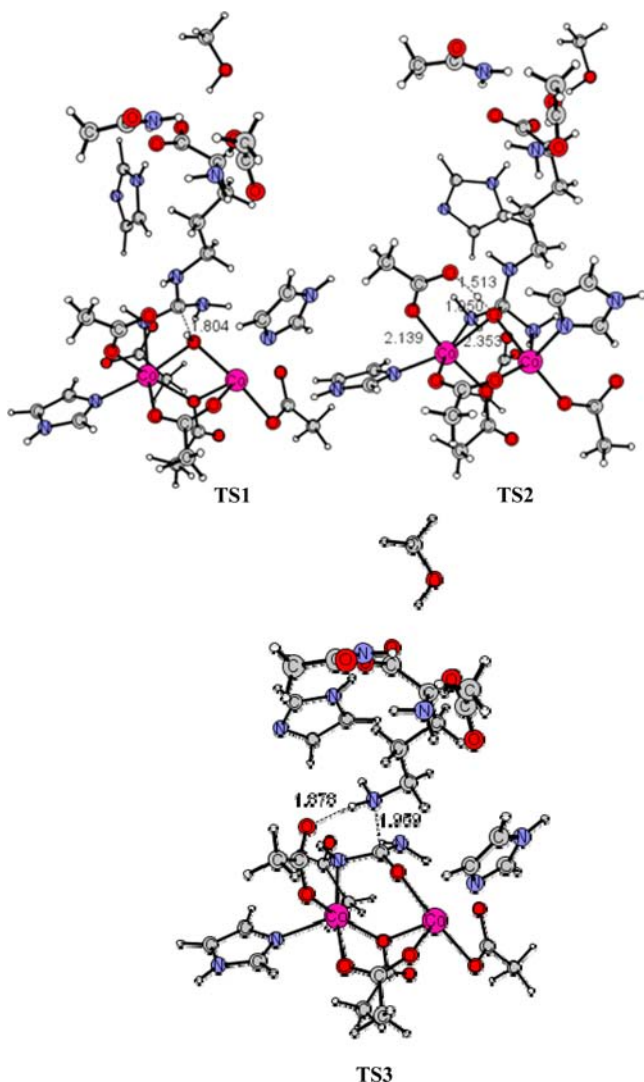


Figure 3. Optimized geometries of the maxima along the reaction pathway. Distances are in angstroms.

barrier height that dictates the rate-limiting steps of the reaction.

The INT1, found at 13.7 kcal/mol, is the tetrahedral intermediate where the short O_H-C distance (1.439 Å) means that the nucleophilic addition is completed. As a consequence, the OH^- group is not tightly bound to the bimetallic center ($OH-Co_A = 2.887$ Å; $OH-Co_B = 2.252$ Å), even if it is still interacting with the Co_B center. This binding mode is not consistent with that proposed to involve metal coordination by the N_ϵ atom of L-Arg¹¹ but is similar to that observed in the tetrahedral boronate anion form of ABH in Co^{2+} -arginase.¹²

The next step corresponds to proton transfer from the $-OH$ group to Asp128 necessary for proton delivery from Asp128 to the N_ϵ atom of Arg. These events are described by TS2 (see Figure 3). The B3LYP functional does not give a correct behavior in the protein environment because higher destabilization of INT1 leads to a relative energy higher than that of TS2. This tendency has been previously noted in other enzymes for the hydrogen-transfer process.^{25,35} For this reason, we have redone the computations by using the Becke88–Becke96–Truhlar2004 (BB1K)³⁷ and Becke96–Adamo98–Truhlar2004 (MPWB1K)³⁸ exchange-correlation functionals, previously used for other enzymes in which this process occurs, because

they give the correct behavior in proton-transfer reactions.^{27,39,40} With respect to INT1, in the TS2 structure, Asp128 and the OH group are closer to Co_A (2.139 and 2.353 Å, respectively). The $N_\epsilon H$ group is differently oriented assuming an almost planar geometry that is more suitable for receiving the proton from Asp128 and, consequently, causing C– N_ϵ bond cleavage of L-Arg. The vibrational motions associated with the imaginary frequency ($147.6i$ cm^{-1}) account for these events. There is INT2 to follow at 7.8 kcal/mol from ES (see Figure 1). At first glance of the optimized geometry of INT2 depicted in Figure 2, it is possible to observe as the proton of the carboxyl group of Asp128 is now on the nitrogen (N_ϵ) of Arg because proton transfer occurs spontaneously during the optimization procedure. The same result has been previously found in the case of the Mn-containing enzyme.¹³ The C–N bond (normally about 1.47 Å) is elongated (1.596 Å), and the C–O bond is shortened (1.345 Å). In order to accomplish the hydrolase action of the enzyme with the achievement of urea and L-Orn as the final products, it is necessary to complete cleavage of the C–N bond. This process occurs throughout TS3 with a barrier of 11.3 kcal/mol in the protein environment. The corresponding optimized geometry is shown in Figure 3. The C–N bond dissociates with an internuclear separation of 1.959 Å, and the calculated imaginary frequency ($147.1i$ cm^{-1}) confirms the dissociation behavior.

In the optimized geometry of the resulting enzyme–product complex (E_p ; Figure 2), both hydrolysis products are retained in the active site by establishing different contacts. In particular, the urea interacts by the carbonyl O atom with Co_B (1.994 Å) and by N_{η^1} with Co_A (2.288 Å). The same arrangement occurred in the case of Mn^{2+} -arginase although with longer distances.

L-Orn is involved in hydrogen bonding with the neighboring residues (Asp128 and His141) and, with its α -amino and α -carboxylate groups, interacts with the Ser137, Asn130, and Asp183 residues. The amino acid side chain is extended into the active site, with the C–C chain adopting a trans conformation. This arrangement is identical with that present in the final product of Mn^{2+} -arginase¹³ and with that found in the corresponding experimental structures,^{12,41} emphasizing that the N_ϵ atom of L-Arg cannot be involved in establishing contacts with metal ions and so cannot assume the orientation hypothesized by Stone et al.¹¹

The interatomic distance between the two Co ions changes during the reaction, suggesting that the flexibility of the active center is guaranteed in the whole catalytic cycle. These variations are small, and the Co–Co bond length is close to the experimentally observed one (3.128 Å).^{4,12,42}

As mentioned previously, the PESs have also been computed by using the BB1K and MPWB1K functionals on the B3LYP-optimized geometries. As shown in Figure 1, these two functionals give similar results along the considered reaction path with energy values lower than that found with B3LYP. Considering that B3LYP generally overestimates the energy barriers in the enzymatic reactions, both the BB1K and MPWB1K functionals seem to confirm better results previously found in many enzymatic reactions.^{27,39,40}

A general comparison between the Co- and Mn-containing arginase evidences that the barriers for the rate-determining step are almost identical, in agreement with the measured experimental k_{cat} values in both enzymes. The differences in K_M can be explained by the computed binding energies in the Michaelis complex (ES).

CONCLUSIONS

In this work, we have studied the reaction mechanism of Co^{2+} -arginase by using the first-principles DFT method, employing different exchange-correlation functionals. Comparing our results with the previous work on Mn^{2+} -arginase, the following conclusions can be drawn: (1) For the Co-containing enzyme, the rate-determining step is the nucleophilic attack of the bridging hydroxide to the substrate C atom. (2) The geometrical parameters as well as the charge distribution in all stationary points are similar in both enzymes. (3) The barriers of the rate-limiting step are almost identical and account for the similar k_{cat} values experimentally measured. (4) The binding energy in the Michaelis complex of Co^{2+} -arginase is slightly higher (about 3 kcal/mol) with respect to the same complex in Mn^{2+} -arginase. This difference can explain in a qualitative manner the different K_{M} values that are experimentally observed.

ASSOCIATED CONTENT

Supporting Information

Cartesian coordinates for all of the species along the reaction path. This material is available free of charge via the Internet at <http://pubs.acs.org>.

AUTHOR INFORMATION

Corresponding Author

*E-mail: tmarino@unical.it. Fax: +39-0984-492014.

Notes

The authors declare no competing financial interest.

ACKNOWLEDGMENTS

The University of Calabria, CASPUR, and MIUR (Grant PRIN 2008F5A3AF_005) are gratefully acknowledged.

REFERENCES

- (1) Daghigh, F.; Fukuto, J. M.; Ash, D. E. *Biochem. Biophys. Res. Commun.* **1994**, *202*, 174–180.
- (2) Boucher, J.-L.; Custot, J.; Vadon, S.; Delaforge, M.; Lepoivre, M.; Tenu, J.-P.; Yapo, A.; Mansuy, D. *Biochem. Biophys. Res. Commun.* **1994**, *203*, 1614–1621.
- (3) Hecker, M.; Nematollahi, H.; Hey, C.; Busse, R.; Racke, K. *FEBS Lett.* **1995**, *359*, 251–254.
- (4) Ash, D. E. *J. Nutr.* **2004**, *2760S*–2764S.
- (5) Hellerman, L.; Perkins, M. E. *J. Biol. Chem.* **1935**, *112*, 175–194.
- (6) Mora, J.; Tarrab, R.; Martuscelli, J.; Soberon, G. *Biochem. J.* **1965**, *96*, 588–594.
- (7) Brown, G. W., Jr. *Arch. Biochem. Biophys.* **1966**, *114*, 184–194.
- (8) Anderson, A. B. *Biochem. J.* **1945**, *39*, 139–142.
- (9) Edlbacher, S.; Baur, H. *Hoppe-Seyler's Z. Physiol. Chem.* **1958**, *254*, 275–284.
- (10) Srivastava, A.; Dwivedi, N.; Samanta, U.; Kumar Sau, A. *IUBMB Life* **2011**, *63* (11), 1027–1036.
- (11) Stone, E. M.; Glazer, E. S.; Chantranupong, L.; Cherukuri, P.; Breece, R. M.; Thierney, D. L.; Curley, S. A.; Iverson, B. L.; Georgiou, G. *ACS Chem. Biol.* **2010**, *5*, 333–342.
- (12) D'Antonio, E. L.; Christianson, D. W. *Biochemistry* **2011**, *50*, 8018–8027.
- (13) Leopoldini, M.; Russo, N.; Toscano, M. *Chem.—Eur. J.* **2009**, *15*, 8026–8036.
- (14) Becke, A. D. *J. Chem. Phys.* **1993**, *98*, 5648–5652.
- (15) Parr, R. G.; Yang, W. *Density-Functional Theory of Atoms and Molecules*; Oxford University Press: Oxford, U.K., 1989.
- (16) Lee, C. T.; Yang, W. T.; Parr, R. G. *Phys. Rev. B: Condens. Matter* **1988**, *37*, 785–789.
- (17) Frisch, M. J.; Trucks, G. W.; Schlegel, H. B.; Scuseria, G. E.; Robb, M. A.; Cheeseman, J. R.; Montgomery, J. A., Jr.; Vreven, T.; Kudin, K. N.; Burant, J. C.; Millam, J. M.; Iyengar, S. S.; Tomasi, J.; Barone, V.; Mennucci, B.; Cossi, M.; Scalmani, G.; Rega, N.; Petersson, G. A.; Nakatsuji, H.; Hada, M.; Ehara, M.; Toyota, K.; Fukuda, R.; Hasegawa, J.; Ishida, M.; Nakajima, T.; Honda, Y.; Kitao, O.; Nakai, H.; Klene, M.; Li, X.; Knox, J. E.; Hratchian, H. P.; Cross, J. B.; Bakken, V.; Adamo, C.; Jaramillo, J.; Gomperts, R.; Stratmann, R. E.; Yazyev, O.; Austin, A. J.; Cammi, R.; Pomelli, C.; Ochterski, J. W.; Ayala, P. Y.; Morokuma, K.; Voth, G. A.; Salvador, P.; Dannenberg, J. J.; Zakrzewski, V. G.; Dapprich, S.; Daniels, A. D.; Strain, M. C.; Farkas, O.; Malick, D. K.; Rabuck, A. D.; Raghavachari, K.; Foresman, J. B.; Ortiz, J. V.; Cui, Q.; Baboul, A. G.; Clifford, S.; Cioslowski, J.; Stefanov, B. B.; Liu, G.; Liashenko, A.; Piskorz, P.; Komaromi, I.; Martin, R. L.; Fox, D. J.; Keith, T.; Al-Laham, M. A.; Peng, C. Y.; Nanayakkara, A.; Challacombe, M.; Gill, P. M. W.; Johnson, B.; Chen, W.; Wong, M. W.; Gonzalez, C.; Pople, J. A. *Gaussian03*, revision C.02; Gaussian, Inc.: Wallingford, CT, 2004.
- (18) Andrae, D.; Häußermann, U.; Dolg, M.; Stoll, H.; Preuß, H. *Theor. Chim. Acta* **1990**, *77*, 123.
- (19) Barone, V.; Cossi, M. *J. Phys. Chem. A* **1998**, *102*, 1995–2001.
- (20) Cossi, M.; Rega, N.; Scalmani, G.; Barone, V. *J. Comput. Chem.* **2003**, *24*, 669–681.
- (21) Siegbahn, P. E. M.; Blomberg, M. R. A. *Chem. Rev.* **2000**, *100*, 421–437.
- (22) Noodleman, L.; Lovell, T.; Han, W. G.; Li, J.; Himo, F. *Chem. Rev.* **2004**, *104*, 459–508.
- (23) Ramos, M. J.; Fernandes, P. A. *Acc. Chem. Res.* **2008**, *41*, 689–698.
- (24) Leopoldini, M.; Marino, T.; Russo, N.; Toscano, M. *Theor. Chem. Acc.* **2008**, *120*, 459–466.
- (25) Chen, S.-L.; Marino, T.; Fang, W.-H.; Russo, N.; Himo, F. *J. Phys. Chem. B* **2008**, *112*, 2494–2500.
- (26) Amata, O.; Marino, T.; Russo, N.; Toscano, M. *J. Am. Chem. Soc.* **2009**, *131*, 14804–14811.
- (27) Alberto, M. E.; Marino, T.; Russo, N.; Ramos, M. J. *J. Chem. Theory Comput.* **2010**, *6*, 2424–2433.
- (28) Amata, O.; Marino, T.; Russo, N.; Toscano, M. *Phys. Chem. Chem. Phys.* **2011**, *13*, 3468–3477.
- (29) Amata, O.; Marino, T.; Russo, N.; Toscano, M. *J. Am. Chem. Soc.* **2011**, *133* (44), 17824–17831.
- (30) Liao, R.-Z.; Himo, F.; Yu, J.-G.; Liu, R.-Z. *J. Inorg. Biochem.* **2010**, *104*, 37–46.
- (31) Alberto, M. E.; Leopoldini, M.; Russo, N. *Inorg. Chem.* **2011**, *50*, 3394–3403.
- (32) Glendenning, E. D.; Reed, A. E.; Carpenter, J. E.; Weinhold, F., NBO, version 3.1.
- (33) Siegbahn, P. E. M.; Himo, F. *Comput. Mol. Sci.* **2011**, *1*, 323–336.
- (34) Chen, S.-L.; Fang, W.-H.; Himo, F. *Theor. Chem. Acc.* **2008**, *120*, 515–522.
- (35) Cox, J. D.; Kim, N. N.; Traish, A. M.; Christianson, D. W. *Nat. Struct. Biol.* **1999**, *6*, 1043–1047.
- (36) Radón, M.; Srebro, M.; Broclawik, E. *J. Chem. Theory Comput.* **2009**, *5*, 1237–1244.
- (37) Zhao, Y.; Truhlar, D. G. *J. Phys. Chem. A* **2004**, *108*, 6908.
- (38) Zhao, Y.; Lynch, B. J.; Truhlar, D. G. *J. Phys. Chem. A* **2004**, *108*, 2715.
- (39) Ribeiro, A. J. M.; Ramos, M. J.; Fernandes, P. A. *J. Chem. Theory Comput.* **2010**, *6*, 2281–2292.
- (40) Sousa, S. F.; Fernandes, P. A.; Ramos, M. J. *J. Phys. Chem. A* **2007**, *111* (42), 10439–10452.
- (41) Di Costanzo, L.; Sabio, G.; Mora, A.; Rodriguez, P. C.; Ochoa, A. C.; Cneteno, F.; Christianson, D. W. *Proc. Natl. Acad. Sci. U.S.A.* **2005**, *102*, 13058–13063.
- (42) Khangulov, S. V.; Pessiki, P. J.; Barynin, V. V.; Ash, D. E.; Dismukes, G. C. *Biochemistry* **1995**, *34*, 2015–2025.